Swarm and Evolutionary Computation 4 (2012) 44–53

Contents lists available at SciVerse ScienceDirect

Swarm and Evolutionary Computation

journal homepage: www.elsevier.com/locate/swevo

Regular paper

State estimation of nonlinear stochastic systems using a novel meta-heuristic particle filter

Mohamadreza Ahmadi [a], Hamed Mojallali [a,*], Roozbeh Izadi-Zamanabadi [b]

[a] Electrical Engineering Department, Faculty of Engineering, University of Guilan, P.O. Box: 3756, Rasht, Iran

[b] Department of Electronic Systems, Automation & Control, Aalborg University, Fredrik Bajers Vej 7, 9220, Aalborg Ø, Denmark

ARTICLE INFO

Article history:
Received 19 April 2011
Received in revised form
26 September 2011
Accepted 21 November 2011
Available online 13 December 2011

Keywords:
Particle filter
Sub-optimal filtering
Nonlinear state estimation
Invasive weed optimization

ABSTRACT

This paper proposes a new version of the particle filtering (PF) algorithm based on the invasive weed optimization (IWO) method. The sub-optimality of the sampling step in the PF algorithm is prone to estimation errors. In order to avert such approximation errors, this paper suggests applying the IWO algorithm by translating the sampling step into a nonlinear optimization problem. By introducing an appropriate fitness function, the optimization problem is properly treated. The validity of the proposed method is evaluated against three distinct examples: the stochastic volatility estimation problem in finance, the severely nonlinear waste water sludge treatment plant, and the benchmark target tracking on re-entry problem. By simulation analysis and evaluation, it is verified that applying the suggested IWO enhanced PF algorithm (PFIWO) would contribute to significant estimation performance improvements.

1. Introduction

State estimation plays a key role in different applications such as fault detection, process monitoring, process optimization, and model based control techniques [1]. Fortunately, a large group of models in signal processing can be represented by a state-space form in which prior knowledge of the system is available. This prior knowledge allows us to exploit a Bayesian estimation approach. Within this statistical framework, one can perform inference on the unknown states according to the posterior distribution. In most cases, the observations arrive sequentially in time, and one is interested in recursively estimating the *hidden* states from the time-varying posterior distribution. This problem is referred as the *optimal filtering* problem [2,3]. Owing to the mathematical complexity, only few specific models (including linear Gaussian state-space models and finite state-space hidden Markov models (HMM) [4]) can be adopted to reach an analytical solution. The popular Kalman filter (KF) [2,3] and the renowned HMM filter [4] provide close form solutions to the latter models.

In many real-life applications, however, the models possess nonlinearity and non-Gaussian behavior. Thus, an optimal solution to the filtering problem cannot be attained. In this case, it becomes necessary to exploit approximate and computationally traceable sub-optimal solutions to the sequential Bayesian estimation methodology. Over the past decades, several sub-optimal filtering methods such as the extended Kalman filter (EKF), and the unscented Kalman filter (UKF) have been proposed in the open literature [5]. But, these filtering algorithms suffer from the *curse of dimensionality*; that is, they perform poorly as the dimension of the model states increases. Furthermore, the rate of convergence of the approximation error decreases dramatically for large state dimensions, say 4 [5]. Notably, it has been demonstrated that the estimation performance of UKF inhibits intrinsic limitations. In other words, the deterministic choice of the so called *sigma points* confines the flexibility desired to construct a probability distribution.

The particle filter (PF), first brought forward by Gordon et al. [6], employs a set of N random samples (or particles) to approximate the posterior distribution. The particles are evolved over time via a combination of importance sampling and re-sampling steps. In a few words, the re-sampling step statistically multiplies and/or discards particles at each time step to adaptively concentrate particles in the regions of high posterior probability [7]. The popularity of the PF results from the notion that it does not call for model simplification or adopting special distributions.

Recently, researchers have shown an increased interest in the subject of integrating meta-heuristic algorithms in PF. In a seminal paper, Tong et al. [8] proposed an optimized PF based on particle swarm optimization (PSO) algorithm [9] which demonstrated improved estimation accuracy. Many subsequent studies also followed the same trend using PSO; e.g., refer

* Corresponding author. Tel.: +98 131 6690276 8; fax: +98 131 6690271.
E-mail addresses: mrezaahmadi@ieee.org (M. Ahmadi), mojallali@guilan.ac.ir (H. Mojallali), riz@es.aau.dk (R. Izadi-Zamanabadi).

2210-6502/$ – see front matter © 2011 Elsevier B.V. All rights reserved.
doi:10.1016/j.swevo.2011.11.004

to [10,11]. In [10], the authors exploited a similar method based on PSO for visual tracking, and claimed that the modified scheme has better accuracy than the conventional PF. Later, Jing et al. [11] further advanced the algorithm brought forward in [8] with a new re-sampling strategy. However, to authors' knowledge, there has been very little discussion on developing other meta-heuristic based PF algorithms, thus far. The studies reported to date have focused on adjusting the PSO enhanced PF algorithm rather than incorporating other techniques established upon evolutionary algorithms and swarm intelligence.

The bio-inspired IWO algorithm was introduced by Mehrabian and Lucas [12] which imitates the colonial behavior of invasive weeds in nature. The IWO algorithm has shown to be virtuous in converging to optimal solution by employing some basic characteristics of weed colonization, e.g. seeding, growth and competition. In [13], Chakraborty et al. investigated the search performance and specifically the effect of population variance on the explorative power of the algorithm. Later, Roy et al. [14] proposed a hybrid optimization algorithm by integrating the optimal foraging theory in IWO which evinced improved optimization capacity. Previously, the IWO algorithm has been utilized in a surfeit of applications including optimizing and tuning of a robust controller [12], antenna configuration optimization [15], optimal arrangement of piezoelectric actuators on smart structures [16], DNA computing [17], and etc.

This paper considers the implementation of the IWO algorithm as a mean to optimize the PF method. Since sampling in PF is carried out in a sub-optimal manner, it can bring about some performance defects such as *sample impoverishment* [5]. By introducing a suitable fitness function for particles, such problems are circumvented and an enhanced PF algorithm is achieved thanks to the IWO approach. The functionality of the combined method is verified using three nonlinear state estimation problems from different fields: volatility estimation of a stock market, state estimation of a nonlinear chemical process, and the re-entry vehicle tracking problem.

The rest of this paper is organized as follows. Section 2 provides a concise description of some preliminary notions including the filtering problem, the Monte Carlo method, Importance Sampling, and the basic particle filtering algorithm. The IWO algorithm is limned in Section 3. The proposed PFIWO method is discussed in Section 4. Simulation Results based on the PFIWO algorithm and some discussions are outlined in Section 5. Section 6 concludes the paper.

2. Preliminaries

2.1. The filtering problem

Consider the general class of nonlinear non-Gaussian systems with state-space model as described below

$$x_k = f(x_{k-1}, u_{k-1}, v_{k-1}), \quad x_k \sim p(x_k|x_{k-1}) \tag{1a}$$

$$y_k = g(x_k, u_k, w_k), \quad y_k \sim p(y_k|x_k), \tag{1b}$$

where the subscript k denotes the time instance. $x_k \in R^{n_x}$ represent the system states with probability distribution of $p(x_k|x_{k-1})$ which is not directly measurable, and $y_k \in R^{n_y}$ is the noise corrupted observation with likelihood $p(y_k|x_k)$. The maps $f \in R^{n_x} \times R^{n_u} \times R^{n_v} \to R^{n_x}$ and $g \in R^{n_x} \times R^{n_u} \times R^{n_w} \to R^{n_y}$ are generally nonlinear functions. u stands for known inputs. v and w represent the process and measurement noise, respectively. The overall structure is illustrated in Fig. 1. *Filtering* is the task of sequentially estimating the states (parameters or hidden variables) of a system as a set of observations become available on-line [2,3]. Strictly speaking, filtering is aimed at estimating the posterior distribution $p(x_k|y_k)$ *as* a set of observations $Y_k = (y_1, y_2, \ldots, y_k)^T$ arrives. It is worth noting that the results obtained in this section are established upon

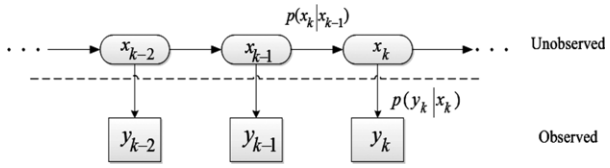

Fig. 1. A graphical representation of the state-space model described by Eq. (1).

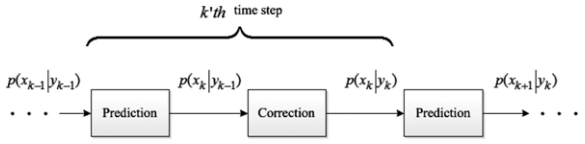

Fig. 2. The Bayesian approach to the filtering problem.

the following assumptions:

1. The states follow a first order Markov process, i.e., $x_k|x_{k-1} \sim p_{x_k|x_{k-1}}(x_k|x_{k-1})$ with an initial distribution of $p(x_0)$.
2. The measurements are conditionally independent given the states, i.e., each y_k only depends on x_k.

The Bayesian solution to the filtering problem consists of two stages [2,3,5]:

1. Prediction: let the above assumptions hold. Using the prior density function, and the Chapman–Kolmogorov equation we have

$$p(x_k|y_{k-1}) = \int p(x_k|x_{k-1})p(x_{k-1}|y_{k-1})dx_{k-1}. \tag{2}$$

2. Correction: based on the Bayes' formula

$$p(x_k|y_k) = \frac{p(y_k|x_k)p(x_k|y_{k-1})}{p(y_k|y_{k-1})} \tag{3a}$$

wherein

$$p(y_k|y_{k-1}) = \int p(y_k|x_k)p(x_k|Y_{k-1})dx_k. \tag{3b}$$

The algorithm is initialized with $p(x_0|y_0) = p(x_0)$ and $p(x_1|y_0) = p(x_1)$. One step operation of the Bayesian filtering is portrayed in Fig. 2. However, it is obvious that achieving a closed form analytical solution to the untraceable integral in Eq. (2) and therefore the solution to Eq. (3) is a cumbersome task. The problem becomes even more severe as the state dimensions increase. Thus, an optimal solution cannot be attained except under very restricting conditions (linear transition functions and Gaussian noise) using the well-known KF. The interested reader can refer to [2,3] which provide a comprehensive theoretical overview of available optimal methods. Sub-optimal solutions exist for rather general models with nonlinear evolution functions and non-Gaussian noises. Nevertheless, due to the nature of these methods (e.g. EKF and UKF) which are based on local linearization, the estimation performance is, more or less, limited. Estimation techniques established upon sequential Monte Carlo methods, namely the PF, are a promising alternative to local linearization algorithms [6,18].

2.2. Monte Carlo and importance sampling techniques

In the Monte Carlo technique, one is concerned with estimating the properties of some highly complex probability distribution $p(x)$, e.g. *expectation*

$$E(s(x)) = \int s(x)p(x)dx \tag{4}$$

where $s(x)$ is some useful function for estimation. In cases where this cannot be obtained analytically, the approximation problem can be handled indirectly. It is possible to represent $p(x)$ by a set

of random samples $\tilde{x}^i,\ i = 1, 2, \ldots, N$. Consequently, the Monte Carlo representation is [16]

$$p(x) = \frac{1}{N}\sum_{i=1}^{N}\delta(x - \tilde{x}^i) \tag{5}$$

where $\delta(.)$ is the Dirac delta function. Then, the expectation can be reformulated as:

$$E(s(x)) = \int s(x)p(x)dx \approx \int s(x)\frac{1}{N}\sum_{i=1}^{N}\delta(x - \tilde{x}^i)dx$$

$$= \frac{1}{N}\sum_{i=1}^{N}s(\tilde{x}^i). \tag{6}$$

Alternatively, suppose that the samples $\tilde{x}^i$ are drawn from a distribution $q(x)$ instead of $p(x)$. Now, the expectation can be estimated using importance sampling as follows:

$$E(s(x)) = \int s(x)p(x)dx = \int s(x)\frac{q(x)p(x)}{q(x)}dx$$

$$\approx \int s(x)\frac{p(x)}{q(x)}\frac{1}{N}\sum_{i=1}^{N}\delta(x - \tilde{x}^i)dx$$

$$= \frac{1}{N}\sum_{i=1}^{N}s(\tilde{x}^i)\frac{p(\tilde{x}^i)}{q(\tilde{x}^i)} = \frac{1}{N}\sum_{i=1}^{N}w_i s(\tilde{x}^i) \tag{7}$$

where $w_i \propto \frac{p(\tilde{x}^i)}{q(\tilde{x}^i)}$ is the importance weight. So, $p(x)$ can be estimated as

$$p(x) = \sum_{i=1}^{N}w_i\delta(x - \tilde{x}^i), \quad \text{s.t.} \sum_{i=1}^{N}w_i = 1. \tag{8}$$

2.3. The basic particle filter

The particle filtering scheme approximates the multi-dimensional integral in the Bayesian prediction and update steps using Monte Carlo sampling. Consider Eqs. (2) and (3), the discussion is followed by reformulating the latter equations based on the Monte Carlo approximation described in the previous section. Let $\tilde{x}^i,\ i = 1, 2, \ldots, N$ be the drawn samples from the posterior distribution $p(x_k|y_k)$. The filter is initialized as [5,18,19]:

$$\tilde{x}_0^j \sim p(x_0|y_0), \quad i = 1, 2, \ldots, N. \tag{9}$$

Then, for $k = 1, 2, \ldots$ we have

$$p(x_k|y_k) = \sum_{i=1}^{N}w_i^k\delta(x - \tilde{x}_k^i), \quad \text{s.t.} \sum_{i=1}^{N}w_i^k = 1. \tag{10}$$

For $i = 1, 2, \ldots, N$ sample from the proposal distribution $q(x_k|x_{k-1})$ as

$$\tilde{x}_k^j \sim q(x_k|\tilde{x}_{k-1}^j). \tag{11}$$

Subsequently, update the importance weights

$$w_i^k = w_i^{k-1}\frac{p(y_k|\tilde{x}_{k-1}^i)p(\tilde{x}_k^i|\tilde{x}_{k-1}^i)}{q(y_k|\tilde{x}_{k-1}^i)}. \tag{12}$$

Provided that $p(x_k|x_{k-1}) = q(x_k|x_{k-1})$, Eqs. (11) and (12) convert to

$$\tilde{x}_k^j \sim p(x_k|\tilde{x}_{k-1}^j) \tag{13a}$$

$$w_i^k = w_i^{k-1}p(y_k|\tilde{x}_{k-1}^i). \tag{13b}$$

Then, for $i = 1, 2, \ldots, N$ normalize the weights

$$w_i^k = \frac{w_i^k}{\sum_{j=1}^{N}w_j^k}. \tag{14}$$

A prevalent problem with PF is the degeneracy phenomenon, wherein after few iterations, all but few particles will have trivial weights. A measure of degeneracy is the effective sample size N_{eff} which can be empirically evaluated as

$$\hat{N}_{\text{eff}} = \frac{1}{\sum_{i=1}^{N}(w_i^k)^2}. \tag{15}$$

The conventional approach to solve around the problem of sample degeneracy is to define a degeneracy threshold N_{th}. If $\hat{N}_{\text{eff}} < N_{\text{th}}$, *re-sampling* should be initiated [7].

3. The invasive weed optimization

3.1. Key terms

Prior to describing the IWO algorithm, the key terms are explained as follows:

a *Seed*: each unit in the colony (here the particles) that encompasses a value for each variable in the optimization problem before fitness evaluation.
b *Weed/Plant*: any seed that is evaluated grows to a weed or plant.
c *Fitness*: a value corresponding to the goodness of each unit after being evaluated.
d *Field*: the search/solution space.
e *Maximum weed population*: a parameter preset representing the maximum number of possible weeds in the field after fitness assessment.

3.2. The IWO algorithm

The process flow of the IWO algorithm is outlined below [14,15]:

1. Initialize the seeds $S_i = (s_1, s_2, \ldots, s_n)^T$, where n is the number of selected variables, over the search space. Thus, each seed contains random values for each variable in the $n - D$ solution space.
2. The fitness of each individual seed is calculated according to the optimization problem, and the seeds grow to weeds able to produce new units.
3. Each individual is ranked based on its fitness with respect to other weeds. Subsequently, each weed produces new seeds depending on its rank in the population. The number of seeds to be created by each weed alters linearly from $N_{\min}$ to $N_{\max}$ which can be computed using the equation given below

$$\text{Number of seeds} = \frac{F_i - F_{\text{worst}}}{F_{\text{best}} - F_{\text{worst}}}(N_{\max} - N_{\min}) + N_{\min}. \tag{16}$$

In which F_i is the fitness of i'th weed. F_{worst}, and F_{best} denote the best and the worst fitness in the weed population. This step ensures that each weed takes part in the reproduction process.
4. The generated seeds are normally distributed over the field with zero mean and a varying standard deviation of σ_{iter} described by

$$\sigma_{\text{iter}} = \left(\frac{\text{iter}_{\max} - \text{iter}}{\text{iter}_{\max}}\right)^n(\sigma_0 - \sigma_f) + \sigma_f \tag{17}$$

where $\text{iter}_{\max}$ and iter are the maximum number of iteration cycles assigned by the user, and the current iteration number, respectively. σ_0 and σ_f represent the pre-defined initial and final standard deviations. n is called the nonlinear modulation index. In order to obtain a full and swift scan of possible values of standard deviation, it has been examined that the most appropriate value for nonlinear modulation index is 3 [15]. The fitness of each seed is calculated along with their parents and the whole population is ranked. Those weeds with less fitness are eliminated through competition and only a number of weeds remain which are equal to *Maximum Weed Population*.

5. The procedure is repeated at step 2 until the maximum number of iterations allowed by the user is reached.

4. The proposed PFIWO algorithm

At the outset of this section, some exclusive features of the IWO algorithm are emphasized. The IWO algorithm certifies that all possible candidates would participate in the reproduction process. In contrast, most meta-heuristic algorithms would not allow the less-fitted individuals to produce offspring such as the GA. Besides, the IWO algorithm is straightforward and it includes less deal of computational burden unlike other methods. As a good illustration, one can consider the PSO algorithm. PSO needs to update both the position and velocity of individuals in each iteration round which require some extra calculations to find the best position in the neighborhood of each particle as well as the whole population. This issue imposes a considerable deal of computational burden.

Having reviewed a number of unique characteristics of IWO, the discussion is proceeded by presenting the proposed PFIWO algorithm. Owing to the fact that the sampling step of the conventional PF is sub-optimal, the IWO is suggested as a means to enhance the sampling step. Here, the goal of the IWO in the sampling step is to trace the particles which correspond to greater weights. Therefore, it is convenient to calculate the fitness of i'th particle as

$$F_i = \frac{p(y_k|\tilde{x}^i_{k-1})p(\tilde{x}^i_k|\tilde{x}^i_{k-1})}{q(y_k|\tilde{x}^i_{k-1})} \tag{18}$$

which in case of $p(x_k|x_{k-1}) = q(x_k|x_{k-1})$ reduces to

$$F_i = p(y_k|\tilde{x}^i_{k-1}). \tag{19}$$

Consequently, the IWO algorithm's task would be to maximize the fitness function. The sampling step is modified as follows:

1. The fitness of each particle is evaluated, and the particles are ranked based on their fitness in the population; i.e., those particles which correspond to greater weights are of higher rank.
2. Perform steps 3, 4, and 5 of the IWO algorithm as described in Section 3 until a predefined number of iteration cycles is reached. It is worth noting that since the basic PF is considerably time-consuming the maximum number of iteration cycles should be chosen as a compromise between estimation performance and algorithm run-time.
3. Subsequently, the weights are updated and normalized using Eqs. (13) and (14).
4. In order to reproduce and pick out the particles with larger weights the re-sampling step is implemented. That is,

$$\{\tilde{x}^i_k, w^k_i\}^N_{i=1} = \left\{\tilde{x}^i_k, \frac{1}{N}\right\}^N_{i=1}. \tag{20}$$

5. Simulation results

In this section, the estimation performance of the proposed PFIWO method is examined and compared with the conventional PF. Three examples are investigated in this section. The first example is devoted to stochastic volatility estimation of a simulated market. The second example considers the state estimation problem of a highly nonlinear chemical process, waste water sludge treatment. Lastly, the performance of both algorithms is challenged with a target tracking on the re-entry problem which has been actively studied as a benchmark for comparing the functionality of several estimation methods.

5.1. The stochastic volatility problem

A prominent group of structures for analyzing volatility are models in which the variance is specified to follow some latent stochastic processes. Such models are referred to as stochastic volatility (SV) models which appear in the theoretical finance literature on option pricing [20–24]. Practical translations of the SV model are classically formulated in discrete time. The canonical model in this class for regularly spaced data is [20,24]

$$x_{t+1} = \mu + \phi(x_t - \mu) + \sigma_\eta \eta_t \quad t \geq 2 \tag{21a}$$

$$h_1 \sim N\left(\mu, \frac{\sigma^2}{1-\phi^2}\right) \tag{21b}$$

$$y_t = e^{\left(\frac{x_t+\mu}{2}\right)}\xi_t \quad t \geq 1 \tag{21c}$$

where superscript t accounts for discrete time in days, and x_t is the unobserved log volatility. y_t denotes the *daily log return* calculated as

$$y_t = \log\left(\frac{S_t}{S_{t-1}}\right) \tag{22}$$

which is earned on stock S between days t and $t-1$. h_t is the log volatility at day t which is assumed to follow a stationary process ($|\phi| < 1$). ξ_t and η_t are uncorrelated Gaussian processes (representing the market shocks) with zero mean and variance of 1. ϕ is the persistence in the volatility, and σ_η signifies the volatility of the *log volatility*. Regarding the economical aspects of the SV model, the interested reader can refer to [20]. Using Eqs. (21) and (22), the financial market corresponding to the parameters listed in Table 1 was simulated. The fluctuations of stock prices are simulated for a time period of 500 days as depicted in Fig. 3. In the first 50 days, the prices grow as the market experiences desirable conditions. From day 51 on, due to say a financial crisis, the stock prices decline dramatically. The daily log return of stock prices is as sketched in Fig. 4. The corresponding volatility is as illustrated in Fig. 5. The PF algorithm as described in Section 2.3. was implemented with 80 particles and the degeneracy threshold was chosen as $N_{\text{th}} = 70$.

One should note that the values for $\text{iter}_{\max}$, $N_{\max}$, and $N_{\min}$ must be selected such that the run-time of the algorithm do not exceed the tolerable range. Moreover, it is important to notice that further incrementing the values for these parameters do not necessarily lead to better results. The initial and final dispersion standard deviations (σ_0 and σ_f) should be adjusted such that the desirable

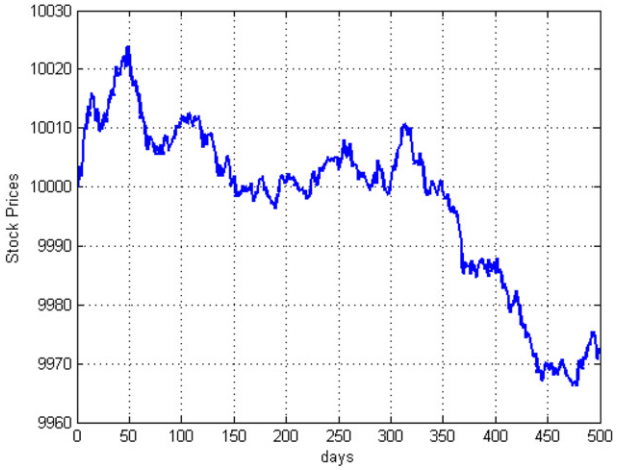

Fig. 3. The fluctuations of the stock prices in the simulated market.

Table 1
The parameter values regarding the simulated stock market.

μ	ϕ	σ	σ_η	S_1
0.1	0.99	0.1	0.05	10 000

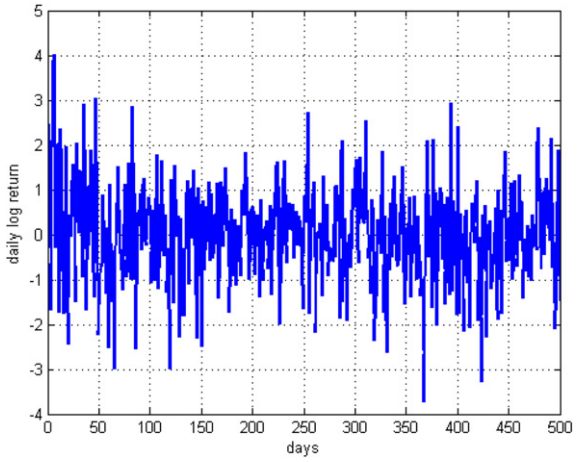

Fig. 4. Daily log return associated with the simulated stock market.

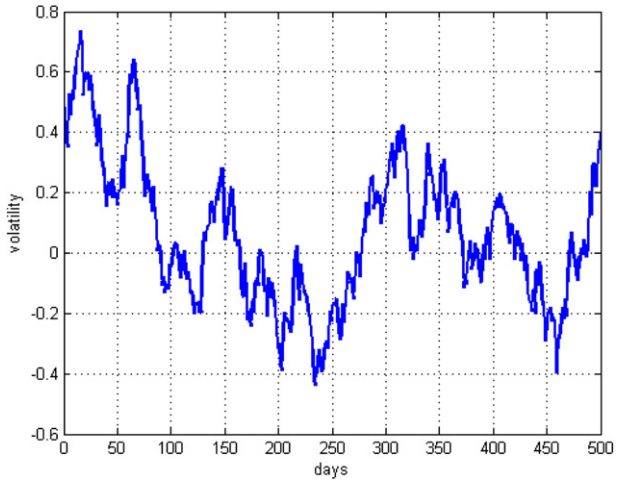

Fig. 5. Resultant stochastic volatility.

Table 2
Parameters used in the PFIWO method for the stochastic volatility problem.

$iter_{max}$	σ_0	σ_f	N_{max}	N_{min}	Max. weed number
20	1	0.001	5	1	50

Table 3
MAPE performance of PF and PFIWO in 10 simulations pertaining to the stochastic volatility problem.

Estimation method	Best (%)	Worst (%)	Mean (%)
PF	1.54	8.61	6.13
PFIWO	0.78	3.39	1.89

Table 4
RMSE performance of PF and PFIWO in 10 simulations pertaining to the stochastic volatility problem.

Estimation method	Best	Worst	Mean
PF	0.1892	2.3471	0.3943
PFIWO	0.0627	0.8154	0.0836

estimation accuracy is reached in regard with $iter_{max}$. All in all, the suitable values of these parameters can be achieved empirically depending on the application.

Having considered the above discussions, the proposed PFIWO method was utilized with the parameters as given in Table 2. The estimated volatility using PF and PFIWO are provided in Fig. 6.

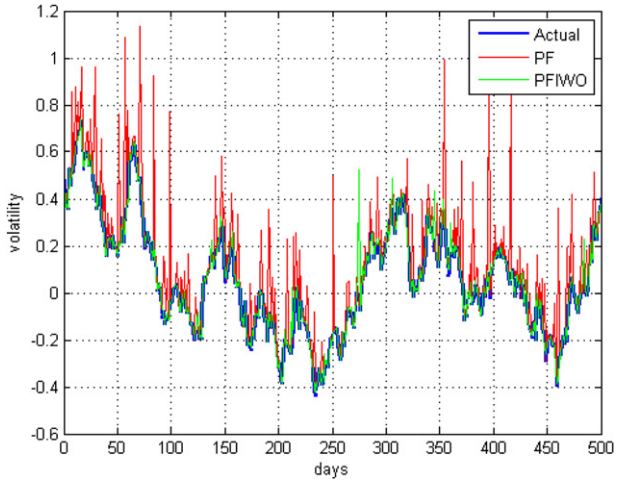

Fig. 6. Volatility estimation results using PF (red) and PFIWO (green). (For interpretation of the references to colour in this figure legend, the reader is referred to the web version of this article.)

As it is observed, except for a peak error at 272th day, the PFIWO has superior estimation performance than the basic PF algorithm. In addition, for the sake of a more reliable comparison, two performance criteria are adopted in this paper: 1. Mean of absolute percentage error (MAPE) defined as

$$\text{MAPE} = \frac{1}{N}\sum_{i=1}^{N}\left|\frac{x(i)-\hat{x}(i)}{x(i)}\right| \tag{23}$$

wherein, x denotes the actual values of states, and $\hat{x}$ signifies the estimated values. 2. Root Mean Square Error (RMSE) given by

$$\text{RMSE} = \sqrt{\frac{1}{N}\sum_{i=1}^{N}(x(i)-\hat{x}(i))^2}. \tag{24}$$

Tables 3 and 4 provide respectively the attained MAPE and RMSE performance of 10 consecutive simulations. From Tables 3 and 4, it can be readily deduced than PFIWO has performed better than PF. In particular, the worst attained state estimates by PFIWO correspond to less total error than those of PF.

5.2. Waste water sludge treatment

State estimation of nonlinear chemical processes is an active research subject [25]. The activated sludge process is one of the most commonly studied biological wastewater treatment methods. In a sludge treatment process, a bacterial biomass suspension (the activated sludge) accounts for the exclusion of contaminants [26]. Overall, the interaction between biomass and substrate is the fundamental part of the treatment process [27]. The interested reader can access a comprehensive review on waste water sludge treatment plants in [28]. The mathematical model used in this study is based on the concept of death-regeneration which has its roots in the work presented in [29]. The following differential equations describe the behavior of the treatment process under endogenous and non-limiting dissolved oxygen conditions in a batch reactor [27]:

$$\dot{S}(t) = -\frac{\lambda}{\theta}\frac{S(t)}{K_s+S(t)}X(t) + k_h\frac{R(t)}{K_x+\frac{R(t)}{X(t)}} \tag{25a}$$

$$\dot{R}(t) = (1-f_p)bX(t) - k_h\frac{R(t)}{K_x+\frac{R(t)}{X(t)}} \tag{25b}$$

Table 5
Parameters used in the PFIWO method for the waste water sludge treatment problem.

$iter_{max}$	σ_0	σ_f	N_{max}	N_{min}	Max. weed number
15	1	0.0001	3	1	80

$$\dot{X}(t) = \lambda \frac{S(t)}{K_s + S(t)} X(t) - bX(t) \tag{25c}$$

$$\dot{P}(t) = f_p bX(t). \tag{25d}$$

The first equation signifies the biodegradable substrate ($S(t)$) dynamics in terms of nonlinear losses resulted from the growth of biomass and production by hydrolysis of slowly biodegradable substrate ($R(t)$). The second equation indicates that the alteration of R is controlled by a fraction of the decay of heterotrophic biomass ($X(t)$) and hydrolysis. In the third equation, the change in biomass caused by decay and growth is formulated. Lastly, the fourth equation characterizes the accumulation of inert material ($P(t)$) as a result of decay of the biomass.

The observation model which subsumes the measurements – endogenous respiration rate (r in mg O_2/l h) and mixed liquor volatile suspended solids (Ω in gCOD/m^3) – and the process states is given by

$$r(t) = \lambda \frac{1-\theta}{\theta} \frac{S(t)}{K_s + S(t)} X(t) \tag{26a}$$

$$\Omega(t) = X(t) + P(t) + R(t). \tag{26b}$$

In order to consider the modeling uncertainties, we adopt a non-Gaussian noise model. Suppose a Gamma probability distribution function given by

$$p(x, \alpha, \beta) = x^{\alpha-1} \frac{e^{-\frac{x}{\beta}}}{\beta^{\alpha}\Gamma(\alpha)} \sim \Gamma(\alpha, \beta) \tag{27}$$

where $\Gamma(.)$ represent the Gamma function, α is the shape parameter, and β is the scale parameter. Let $\alpha = 2$, and $\beta = 5$. This density function is used to characterize the noise associated with the model dynamics. Therefore, a noise signal is generated using the probability distribution given by Eq. (27) and added to each process state. Moreover, in order to take into account sensor errors, two Gaussian noise processes ($N(0, 0.5)$) were generated and added to the measurements. The values for different parameters associated with the measurement and process model are as follows [26]: $S(0) = 100$ mg/l, $R(0) = 100$ mg/l, $X(0) = 1500$ mg/l, $P(0) = 100$ mg/l, $\theta = 0.67$, $\lambda = 0.17$ l/h, $b = 0.025$ l/h, $k_h = 0.1$ l/h, $K_s = 20$ mg/l, $K_X = 0.02$ mg/l, and $f_p = 0.08$.

The differential equations (25a)–(25d) were simulated based on the Euler–Maruyama method. Since $S(t)$ and $R(t)$ possess relatively faster dynamics than the other two states, they were simulated and estimated in a time period of 2 h using the Euler–Maruyama method; whereas, $X(t)$ and $P(t)$ were simulated in the time span of 200 h. It should be noted that in all cases 200 data samples were used. Consequently, the Euler step in the first set of simulations was set to 0.01 h, and in the second round was adjusted to 1 h. Based on the models and the introduced noises, a state estimation simulation was performed. The number of particles in the PF algorithm was preset to 100, while the number of particles for the PFIWO algorithm was set to 80. The remaining parameters regarding the proposed PFIWO methodology are presented in Table 5. The estimated states are depicted in Fig. 7, and the estimation errors associated with each method are portrayed in Fig. 8. Note that due to the extreme nonlinearity of the state-space model and the non-Gaussian nature of the associated process noise, PF is not able to completely follow the state fluctuations. Clearly, PFIWO has led to greater state approximation accuracy. Furthermore, the corresponding RMSE and MAPE values for different states in 10 simulations are provided in Tables 6 and 7. Again, it can be observed that the state estimation errors from the PFIWO algorithm are considerably lower than those of PF. We remark that the number of particles has been augmented to 200 in order to arrive at a more reasonable justification.

5.3. Tracking a ballistic object on re-entry

This section considers the re-entry tracking problem, where a ballistic object enters the atmosphere at high altitude and at a very high speed. The position of the object is tracked by a radar system which measures the range and the bearing. This problem has been addressed by a number of papers [30–32] on nonlinear filtering, since the forces which affect the object possess strong nonlinearities and are a challenge to any filtering method. There are three major forces in effect. The chief force in operation is aerodynamic drag, which is a function of object speed and has a considerable nonlinear variation in altitude. The second one is the gravity, which accelerates the object toward the center of the earth. The remaining forces are random buffeting terms [30]. Under such forces, the trajectory of the object is almost ballistic at the beginning. But, as the density of the atmosphere increases, drag effects become important and the object decelerates rapidly until its motion becomes almost vertical. The state-space model for the system described above can be characterized as follows [31]:

$$\dot{x}_1(t) = x_3(t) \tag{28a}$$

$$\dot{x}_2(t) = x_4(t) \tag{28b}$$

$$\dot{x}_3(t) = D(t)x_3(t) + G(t)x_1(t) + \omega_1(t) \tag{28c}$$

$$\dot{x}_4(t) = D(t)x_4(t) + G(t)x_2(t) + \omega_2(t) \tag{28d}$$

$$\dot{x}_5(t) = \omega_3(t) \tag{28e}$$

Table 6
MAPE performance of PF and PFIWO in 10 simulations pertaining to the wastewater sludge treatment problem.

Estimation method	Best				Worst				Mean			
	R (%)	S (%)	X (%)	P (%)	R(%)	S (%)	X (%)	P (%)	R (%)	S (%)	X (%)	P (%)
PF	8.34	9.92	11.34	13.46	20.32	18.49	28.11	28.67	10.72	12.06	28.11	28.67
PFIWO	2.91	2.98	1.83	2.02	6.74	5.47	7.56	4.15	3.07	3.49	2.55	2.63

Table 7
RMSE performance of PF and PFIWO in 10 simulations pertaining to the wastewater sludge treatment problem.

Estimation method	Best				Worst				Mean			
	R	S	X	P	R	S	X	P	R	S	X	P
PF	0.9629	1.7195	0.9284	1.8132	4.3842	4.0377	3.1937	4.3846	2.7203	2.1483	1.5355	2.0018
PFIWO	0.0387	0.0984	0.0742	0.0661	2.3721	1.0378	2.0469	1.6032	0.0822	0.1105	0.5997	0.3471

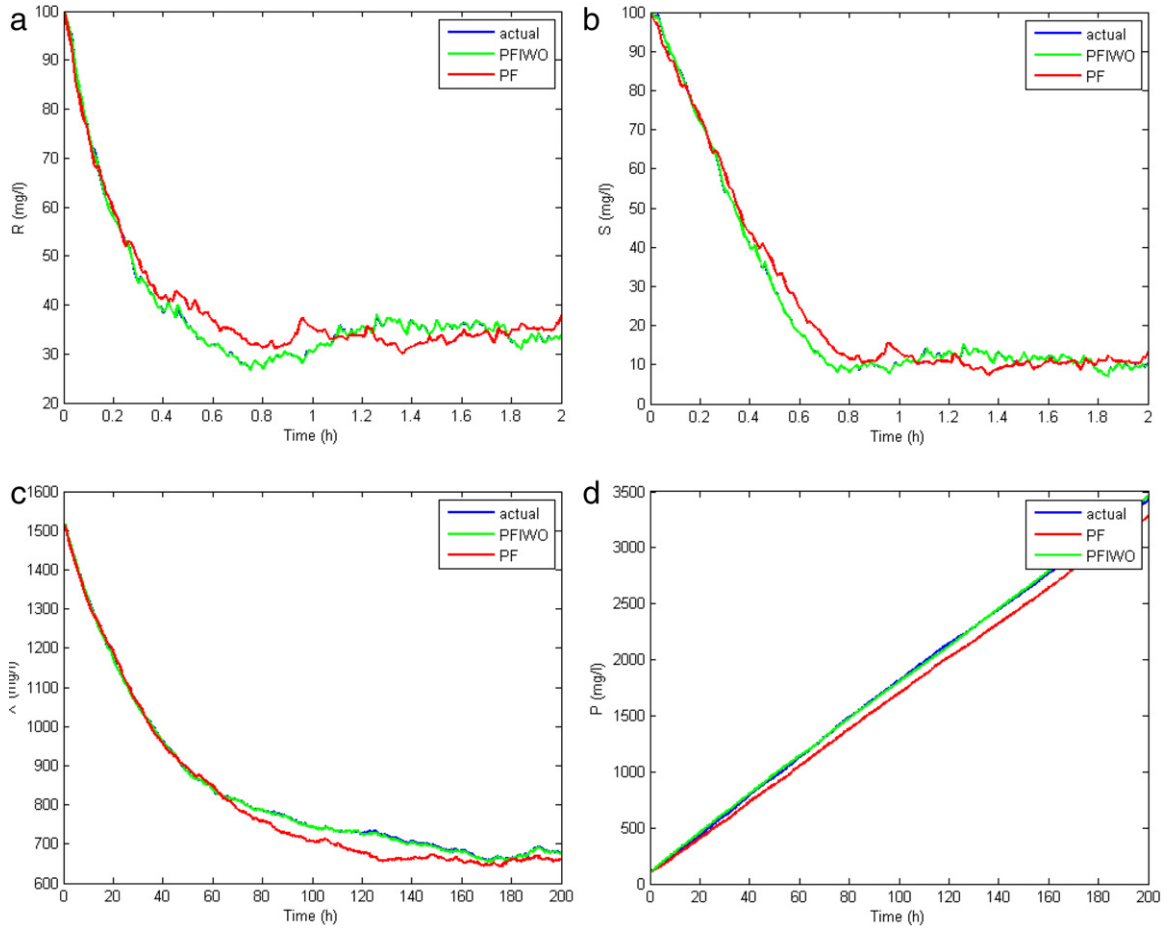

Fig. 7. The estimated states (a) R, (b) S, (c) X, and (d) P.

wherein x_1 and x_2 denote the position of the object in two dimensional space, x_3 and x_4 are the velocity components, and x_5 is a parameter associated with the object's aerodynamic properties. $D(t)$ and $G(t)$ are the drag-related and gravity-related force terms, respectively. $\omega_i(t)$, $i = 1, 2, 3$ are the process noise vectors. The force terms can be calculated as

$$D(t) = \beta(t) \exp\left(\frac{R_0 - R(t)}{H_0}\right) V(t) \tag{29a}$$

$$G(t) = -\frac{G_{m_0}}{R^3(t)} \tag{29b}$$

$$\beta(t) = \beta_0 \exp\left(x_5(t)\right) \tag{29c}$$

where $R(t) = \sqrt{x_1^2(t) + x_2^2(t)}$ is the distance from the center of the earth and $V(t) = \sqrt{x_3^2(t) + x_4^2(t)}$ is the object speed. The radar (which is located at $(R_0, 0)$) is able to measure r (range) and θ (bearing) at a frequency of 10 Hz as follows

$$r = \sqrt{(x_1(t) - R_0)^2 + x_2(t)^2} + \xi_1(t) \tag{30a}$$

$$\theta = \arctan\left(\frac{x_2(t)}{x_1(t) - R_0}\right) + \xi_2(t) \tag{30b}$$

where $\xi_1(t)$ and $\xi_2(t)$ are zero-mean uncorrelated noise processes with variances of 1 m and 17 m rad s [30,31]. Let the simulated discrete process covariance be [32]

$$Q(k) = \begin{bmatrix} 2.4064 \times 10^{-5} & 0 & 0 \\ 0 & 2.4064 \times 10^{-5} & 0 \\ 0 & 0 & 10^{-6} \end{bmatrix}. \tag{31}$$

The values for different constants are set as [31]

$$\beta_0 = -0.59783$$
$$H_0 = 13.406$$
$$G_{m_0} = 3.9860 \times 10^5$$
$$R_0 = 6374. \tag{32}$$

The stochastic differential equations (28a)–(28e) was simulated using 2000 steps of the Euler–Maruyama method with $\Delta t = 0.1$ s. The number of particles was set to 1500 which is relatively low for a target tracking problem. The main reason for this choice is to demonstrate the ability of the PFIWO method to estimate the states of the ballistic object with less number of particles where PF cannot reach an acceptable result. The degeneracy threshold N_{th} was selected as 1200, and a systematic re-sampling scheme [7] has been chosen for the PF method. The parameters of the PFIWO algorithm are given in Table 8. Note that the *Max. Weed Number* should be equal to the number of particles, as it is the case in all of the preceding examples. The target tracking results obtained using the PF and PFIWO methodologies are depicted in Fig. 9. The corresponding tracking errors are also provided in Figs. 10 and 11. As it is observed from the figures, when the PFIWO scheme is used, the tracking errors are in the satisfactory range and PFIWO is capable of tracking the object's trajectory. On the other hand, large state estimation errors result as the traditional PF algorithm is utilized. It is obvious that the deteriorated estimation accuracy of PF is a consequence of the number of particles, whereas the proposed PFIWO method has preserved its approximation performance with the same number of particles. Moreover, the number of particles has been increased to 3000 and the same

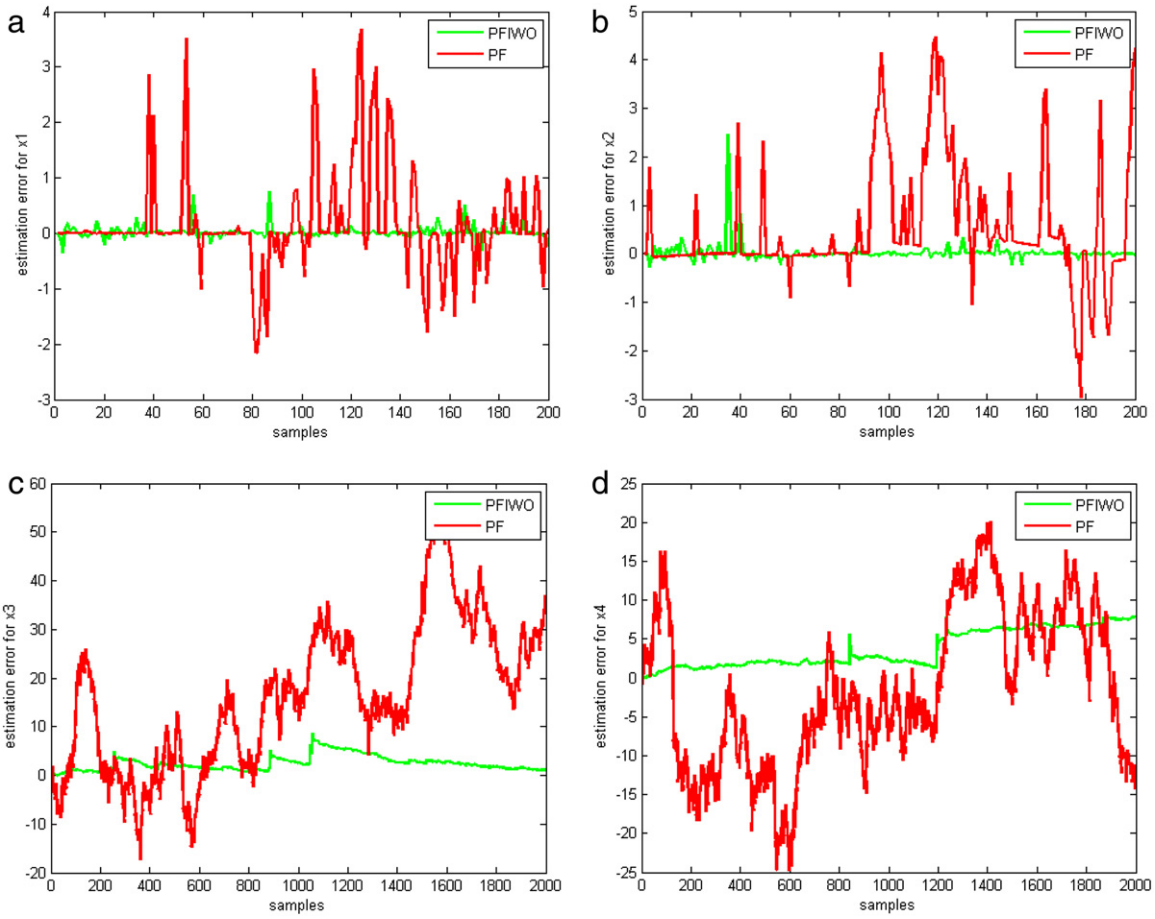

Fig. 8. The corresponding estimation errors for (a) X, (b) R, (c) S, and (d) P.

Table 8
Parameters used in the PFIWO method for the re-entry target tracking problem.

$\text{iter}_{\max}$	σ_0	σ_f	$N_{\max}$	$N_{\min}$	Max. weed number
15	0.1	0.000001	4	1	1500

Table 9
MAPE performance of PF and PFIWO in 10 simulations pertaining to the re-entry target tracking problem.

Estimation method	Best		Worst		Mean	
	x_1 (%)	x_2 (%)	x_1 (%)	x_2 (%)	x_1 (%)	x_2 (%)
PF	5.47	7.36	12.73	10.48	7.53	8.04
PFIWO	2.89	2.36	5.15	6.03	3.33	4.62

Table 10
RMSE performance of PF and PFIWO in 10 simulations pertaining to the re-entry target tracking problem.

Estimation method	Best		Worst		Mean	
	x_1	x_2	x_1	x_2	x_1	x_2
PF	0.8947	0.9257	2.7435	3.1783	1.0074	1.2715
PFIWO	0.1745	0.1011	0.9882	0.9917	0.3078	0.4822

simulations have been launched 10 times. The resultant MAPE and RMSE errors are portrayed in Tables 9 and 10. Once more as expected, the results sketched in these tables corroborate the claim that PFIWO results in significant less state approximation error.

Taken together, the obvious finding that emerges from the set of simulations given in this section is that the proposed PFIWO method can be applied as a powerful state estimation algorithm in case of model nonlinearity and in the presence of non-Gaussian noises.

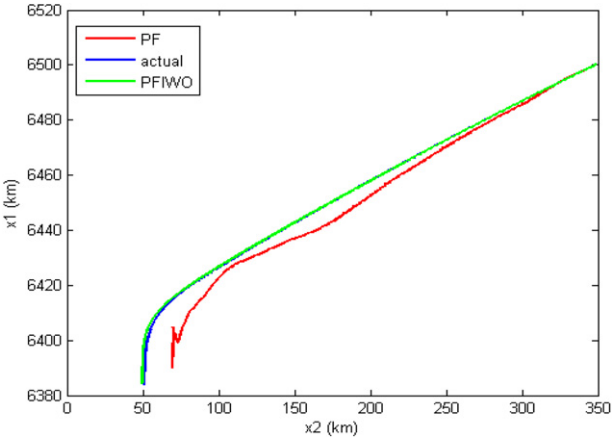

Fig. 9. Tracking performance of PF and PFIWO.

6. Conclusions

An enhanced PF algorithm established upon the IWO scheme is proposed. Firstly, the sampling step is transformed to an optimization problem by defining an apt fitness function. Then, the IWO algorithm is exploited to deal with the optimization problem efficiently. The results based on the proposed methodology are

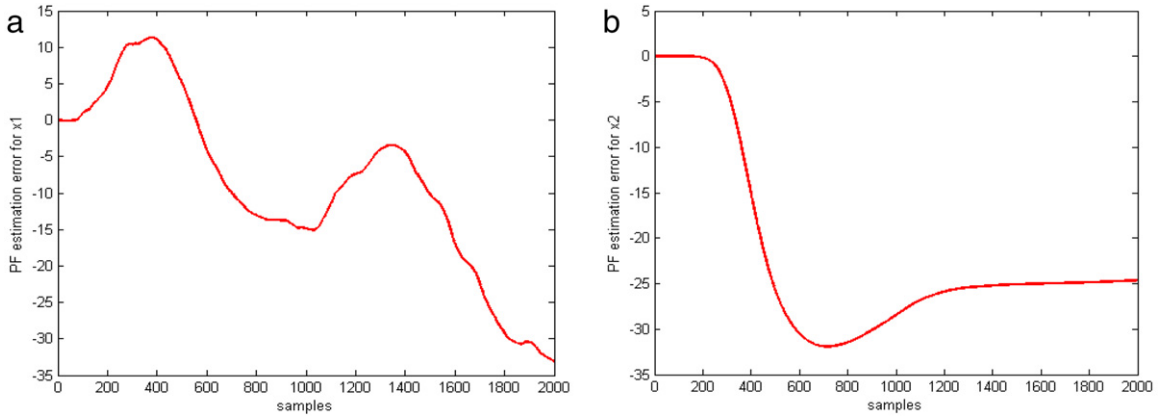

Fig. 10. PF tracking errors for (a) x_1 and (b) x_2.

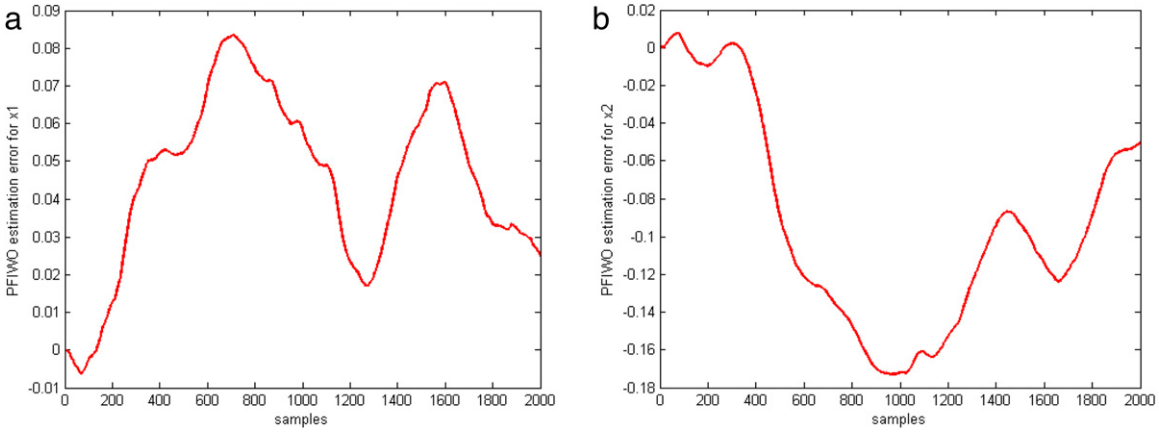

Fig. 11. PFIWO tracking errors for (a) x_1 and (b) x_2.

supplemented which verifies the algorithm's accuracy. It is, therefore, demonstrated that the proposed algorithm can be used for state estimation of highly nonlinear plants. Furthermore, it is also shown, through simulations, that the PFIWO algorithm is robust against the shortcomings of the conventional PF.

References

[1] R. Kandpu, B. Foss, L. Imsland, Applying the unscented Kalman filter for nonlinear state estimation, Journal of Process Control 18 (7–8) (2008) 753–768.
[2] B.D.O. Anderson, J.B. Moore, Optimal Filtering, Prentice Hall, 1979.
[3] T. Kailath, A. Sayed, B. Hassibi, Linear Estimation, Prentice Hall, 2000.
[4] R.J. Elliott, L. Aggoun, J.B. Moore, Hidden Markov Models: Estimation and Control, third ed., Springer-Verlag, 2008.
[5] B. Ristic, M. Arulampalam, A. Gordon, Beyond Kalman Filters: Particle Filters for Tracking Applications, Artech House, 2004.
[6] N. Gordon, D. Salmond, A.F. Smith, A novel approach to nonlinear/non-Gaussian Bayesian estimation, IEE Proceedings F, Radar and Signal Processing 140 (2) (1993) 107–113.
[7] R. Doucet, O. Cappe, E. Moulines, Comparison of resampling schemes for particle filtering, in: 4th international Symposium on Image and Signal Process and Analysis, ISPA, Zagreb, Croatia, 2005.
[8] G. Tong, Z. Fang, X. Xu, A particle swarm optimized particle filter for nonlinear system state estimation, in: IEEE Congress on Evolutionary Computing, 2006, pp. 438–442.
[9] R. Poli, J. Kennedy, T. Blackwell, Particle swarm optimization: an overview, Swarm Intelligence 1 (1) (2007) 33–57.
[10] J. Zhao, Z. Li, Particle filter based on particle swarm optimization re-sampling for vision tracking, Expert Systems with Applications 37 (12) (2010) 8910–8914.
[11] W. Jing, H. Zhao, C. Song, D. Liu, An optimized particle filter based on PSO algorithm, in: International Conference on Future BioMedical Information Engineering, 2009, pp. 122–125.
[12] A.R. Mehrabian, C. Lucas, A novel numerical optimization algorithm inspired from weed colonization, Ecological Informatics 1 (4) (2006) 355–366.
[13] P. Chakraborty, G.G. Roy, S. Das, B.K. Panigrahi, On population variance and explorative power of invasive weed optimization algorithm, in: World Congress on Nature and Biologically Inspired Computing, NaBIC 2009, IEEE Press, Coimbatore, India, 2009.
[14] G.G. Roy, P. Chakraborty, S.-Z. Zhao, S. Das, P.N. Suganthan, Artificial foraging weeds for global numerical optimization over continuous spaces, in: IEEE Congress on Evolutionary Computation, 2010, pp. 1–8.
[15] S. Karimkashi, A.A. Kishk, Invasive weed optimization and its features in electromagnetic, IEEE Transactions on Antennas and Propagation 58 (4) (2010) 1269–1278.
[16] A.R. Mehrabian, A. Yousefi-Koma, A novel technique for optimal placement of piezoelectric actuators on smart structures, Journal of the Franklin Institute 348 (1) (2009) 12–23.
[17] X. Zhang, Y. Wang, G. Cui, Y. Niu, J. Xu, Application of a novel IWO to the design of encoding sequences for DNA computing, Computers and Mathematics with Applications 57 (11–12) (2009) 2001–2008.
[18] H.R. Kunsch, Recursive Monte Carlo filters: algorithms and theoretical analysis, Annals of Statistics 33 (5) (2005) 1983–2001.
[19] A. Doucet, N. De Freitas, N. Gordon, Sequential Monte Carlo Methods in Practice, Springer, New York, 2001.
[20] J. Hull, A. White, The pricing of options on assets with stochastic volatilities, The Journal of Finance 42 (2) (1987) 281–300.
[21] Y. Zheng, Estimating stochastic volatility via filtering for the micromovements of asset prices, IEEE Transactions on Automatic Control 49 (3) (2004) 338–348.
[22] H. Chen, Estimating stochastic volatility using particle filters, M.Sc. Thesis, Case Western Reserve University, 2009.
[23] S. Kim, N. Shepherd, S. Chib, Stochastic volatility: likelihood inference and comparison with ARCH mModels, The Review of Economic Studies 65 (3) (1998) 361–393.
[24] E. Ghysels, A.C. Harvey, E. Renault, Stochastic volatility, in: C.R. Rao, G.S. Maddala (Eds.), Statistical Methods in Finance, North-Holland, Amsterdam, 1996, pp. 119–191.
[25] W. Chen, Bayesian estimation by sequential Monte Carlo sampling, Ph.D. Thesis, Ohio State University, 2004.
[26] M.B. Beck, Identification, estimation, and control of biological waste-water treatment processes, IEE Proceedings D, Control Theory and Applications 133 (5) (1986) 254–264.
[27] K.J. Keesman, State and parameter estimation in biotechnical batch reactors, Control Engineering Practice 10 (2002) 212–225.

[28] K.V. Gernaey, M.C.M. van Loosdrecht, M. Henze, M. Lind, S.B. Jorgensen, Activated sludge waste-water treatment plant modeling and simulation: state of the art, Environmental Modelling and Software 19 (2004) 763–783.
[29] K.J. Keesman, H. Spanjers, G. van Straten, Analysis of endogenous process behavior in activated sludge, Biotechnology and Bioengineering 57 (2) (2000) 155–163.
[30] P.J. Costa, Adaptive model architecture and extended Kalman–Bucy filters, IEEE Transactions on Aerospace and Electronic Systems 30 (1994) 525–533.
[31] S.J. Julier, J.K. Uhlmann, Corrections to unscented filtering and nonlinear estimation, Proceedings of the IEEE 92 (2004) 1958–1958.
[32] S. Sarkka, On unscented Kalman filtering for state estimation of continuous-time nonlinear systems, IEEE Transactions on Automatic Control 52 (9) (2007) 1631–1640.